THE JOURNAL OF PHYSICAL CHEMISTRY Letters

Letter

Cite This: J. Phys. Chem. Lett. 2017, 8, 5626-5632

pubs.acs.org/JPCL

Strong Coupling between Self-Assembled Molecules and Surface Plasmon Polaritons

J. Bigeon,[†] S. Le Liepvre,[‡] S. Vassant,[‡] N. Belabas,[†] N. Bardou,[†] C. Minot,[†] A. Yacomotti,[†] A. Levenson,[†] F. Charra,[‡] and S. Barbay*[,†]

[†]Centre de Nanosciences et de Nanotechnologies, CNRS, Université Paris-Sud, Université Paris-Saclay, C2N Marcoussis, 91460 Marcoussis, France

[‡]Service de Physique de l' État Condensé, SPEC-CEA, CNRS, Université Paris-Saclay, CEA Saclay, F-91191 Gif-sur-Yvette, France

ABSTRACT: We experimentally demonstrate strong coupling between self-assembled PTCDI-C7 organic molecules and the electromagnetic mode generated by surface plasmon polaritons (SPPs). The system consists of a dense self-assembly of ordered molecules evaporated directly on a thin gold film, which stack perpendicularly to the metal surface to form H-aggregates, without a host matrix. Experimental wavevector-resolved reflectance spectra show the formation of hybrid states that display a clear anticrossing, attesting the strong coupling regime with a Rabi splitting energy of $\Omega_R \simeq 102$ meV at room temperature. We demonstrate that the strength of the observed strong coupling regime derives from the high degree of organization of the dense layers of self-assembled molecules at the nanoscale that results in the concentration of the oscillator strength in a charge-transfer Frenkel exciton, with a dipole moment parallel to the direction of the maximum electric field. We compare our results to numerical simulations of a transfer matrix model and reach good qualitative agreement with the experimental findings. In our nanophotonic system, the use of self-assembled molecules opens interesting prospects in the context of strong coupling regimes with molecular systems.

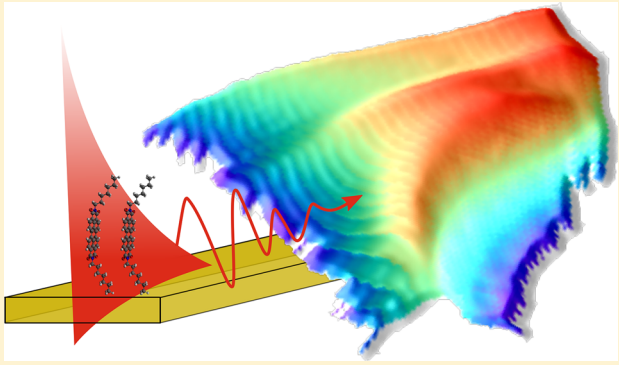

Plasmonic systems in an "open-cavity" architecture have been shown to interact in the strong coupling regime with a variety of organic materials as optical dipoles at room temperature.[1,2] In the strong coupling regime, light−matter interaction modifies substantially the coupled system energy spectrum and gives rise to hybrid states. An ultrastrong coupling regime, where the Rabi splitting is of the same order of magnitude as the frequency of the oscillator and of the field, has also been reported in molecular systems.[3] Plasmonic open cavities with organic molecules are thus appealing for potential applications of strong coupling, such as low threshold lasing and polariton condensation,[4] or ultrafast light amplification[5,6] because of their simplicity and the possibility to operate at room temperature. By their properties of efficient luminescence, low Stokes shift, and large oscillator strength, J-aggregates of organic dye molecules have been widely studied.[7] In these systems, the molecules are usually spin-coated or evaporated in amorphous or nanocrystalline thin layers and dispersed in a host matrix. The strong coupling regime necessitates the use of small confined mode-field volumes V and large oscillator strengths f because the dipole−photon coupling scales as $\sqrt{f/V}$.[8] Surface plasmon polariton (SPP) fields in open-cavity architectures offer nanoscale mode confinement with a resonant enhancement of the field at the SPP resonance. In addition, high densities of coherently oscillating chromophores can lead to large effective dipole moments, increasing the coupling proportionally to the square root of the number of coherent oscillators in the mode volume,[7] thereby making the observation of the strong coupling regime easier in absorption measurements. By contrast, spontaneous emissions from different excited states are noncoherent, and the manifestation of strong coupling relies on oscillator strengths. Large oscillator strengths can however be obtained through dipole−dipole interaction among adjacent molecules, possibly mediated by surface plasmons,[9,10] which leads to delocalized excitonic transitions involving many molecules as in J-aggregates of, e.g., cyanine dyes. However, with low Stokes shifts, the luminescence is emitted in the low-energy strongly coupled plasmon Franck−Condon exciton, corresponding to the absorption line.[1] This raises the question of the role of this strong coupling for large Stokes shifts such as those found in H-aggregates.

Large molecule−field coupling is favored by high molecular densities but also by the alignment of molecular dipole moments along the local electric field vector. Self-assembled molecules can offer a convenient strategy to achieve well-ordered dipoles at the molecular scale. In contrast with polymer matrix approaches, self-organization processes lead to the

Received: September 29, 2017
Accepted: November 2, 2017
Published: November 2, 2017

DOI: 10.1021/acs.jpclett.7b02586
J. Phys. Chem. Lett. 2017, 8, 5626−5632

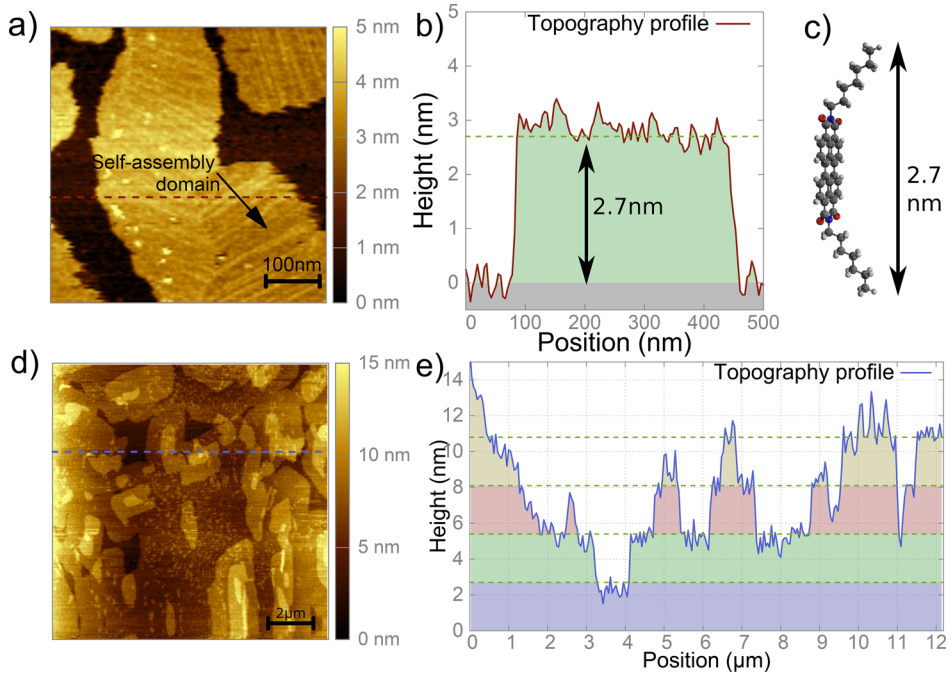

Figure 1. (a) AFM topographic image of a self-assembled monolayer of molecules revealing growth domains with different orientations. (b) Corresponding height profile (along red dashed line), which confirms the deposition of molecules standing on the substrate, as sketched in (c). (d) AFM topographic image of 11 layers of PTCDI-C7 molecules evaporated on a gold thin film. (e) Height profile along the blue dashed line showing height jumps corresponding to a single monolayer.

formation of ultradense and robust arrays of molecules with designed molecular orientation on a variety of large-area substrates.[11] In addition, this approach allows the creation of out-of-plane functions and avoids the proximity of conducting substrates resulting in Dexter quenching of electronic excitations.[12] Furthermore, self-organization processes interacting with the SPP field provide effective methods to maximize the number of dipole moments in interaction with the plasmon field in the mode volume of the SPP.[13] Consequently, a self-assembly approach opens interesting prospects to tune the strength of the plasmon−exciton coupling at the nanoscale and makes an important step toward fully integrated systems in nanophotonics.

In this work, we demonstrate plasmon−exciton coupled states between ultradense self-assembled dyes (*N*,*N*′-diheptyl-3,4,9,10-perylenedicarboximide, hereafter denoted PTCDI-C7) in two-dimensional (2D) structures with a large Stokes shift and SPP on a gold thin film. This Letter is organized as follows. First, we report the formation of H-aggregates of PTCDI-C7 by self-assembly. Then, we address the strong coupling process between the self-assembled molecules and SPPs by experimental investigations in absorption with leakage radiation microscopy (LRM).[14] We demonstrate the spectral and orientational roles of organization of PTCDI-C7 molecules. We numerically model this hybrid systems by a transfer matrix approach. Last, we investigate light emission coupled to SPP modes.

Organic dyes such as PTCDI molecules and their derivatives have been widely used as organic semiconductors[15] and have been shown to self-assemble as highly ordered layers on different types of substrates.[16] Here, we investigate the self-organization processes of PTCDI-C7 molecules, which present a planar PTCDI dye to which are attached two C7 arms on the *N* position, forming an overall structure about 2.7 nm in height.

In this experiment, PTCDI-C7 molecules were evaporated monolayer by monolayer on the top of a thin gold film (40 nm thickness) deposited on a SiO_2 coverslip. We show in Figure 1 the topographic study of a single-monolayer thin film and of a 30 nm thick (11 layers) film obtained by atomic force microscopy (AFM) operated in a noncontact (tapping) mode. The topographic image presented in Figure 1a clearly displays growth domains with molecular arrangements oriented along different directions. In Figure 1b, we note that the thickness of the stepwise domains is always equal to the total length of the PTCDI-C7 molecules (2.7 nm), as shown in Figure 1c. This is an indication that the molecules are stacked together perpendicularly to the gold surface. From the deposited weight forming one monolayer, the density of molecules is estimated to around 9 molecules/nm^2.

We now consider the sample corresponding to the deposition of a 30 nm thick film of PTCDI-C7 molecules. The AFM image in Figure 1d shows crystalline aggregates of PTCDI-C7 as reported in the literature.[16,17] The average size of the crystalline islands is around 250 nm, with a root-mean-square (rms) roughness of 2 nm. Height profiles along dashed line have been extracted from the AFM topography and reported in Figure 1e. Profiles show a mostly flat terraced surface forming two-dimensional islands. Starting from an area forming a flat plateau, the profile fluctuates in integer values of the PTCDI-C7 molecule height (2.7 nm), represented by the dashed lines. These arrangements and figures are in good agreement with crystallographic data acquired on crystals and lamellar mesophases of several alkylated PTCDIs, including PTCDI-C7.[18] Consequently, we can assume essentially a layer-by-layer growth process with molecular orientation perpendicular to the gold thin film resulting in a highly ordered structure.

The photophysics of the evaporated molecules have been studied by absorption and photoluminescence experiments

DOI: 10.1021/acs.jpclett.7b02586
J. Phys. Chem. Lett. 2017, 8, 5626−5632

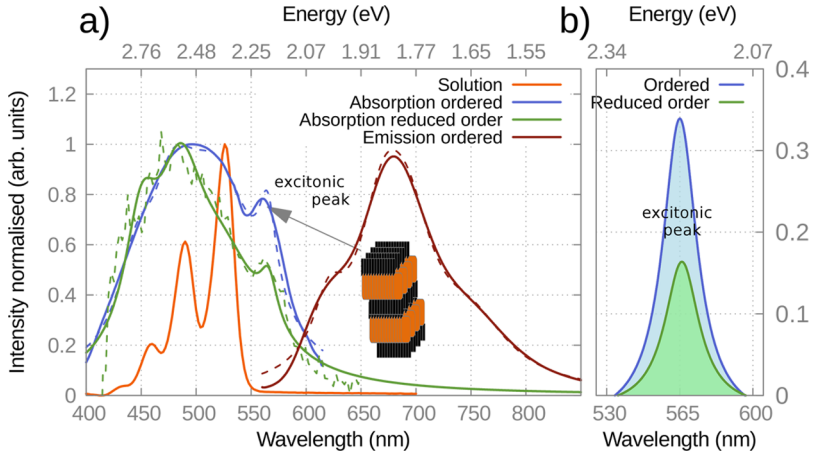

Figure 2. (a) Normalized absorption spectra of PTCDI-C7 molecules dispersed in toluene solution (orange), and of a film composed of ∼30 nm of ordered (blue) and reduced order (green) PTCDI-C7 self-assembled molecules; (inset) sketch of the molecular lamellar organization in the layer; Normalized photoluminescence spectrum recorded under laser excitation at λ = 532 nm for the well-ordered molecules (red). Absorption and emission lines (dashed) are fitted (full lines) with Lorentzian profiles (gray). (b) Excitonic peak in absorption at 565 nm from a fitted Lorentzian profile for self-assembled ordered (blue) and reduced order (green) PTCDI-C7 molecules.

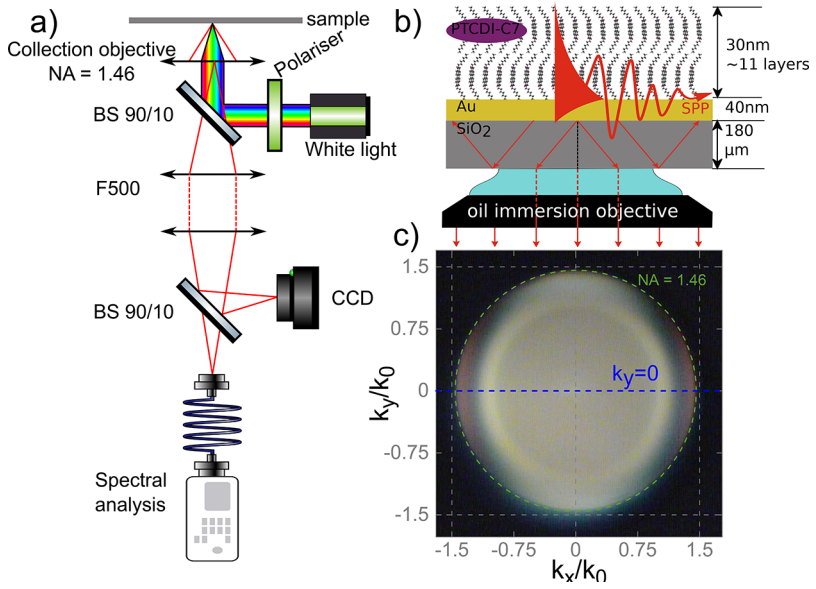

Figure 3. (a) Sketch of the experimental LRM setup based on a high numerical aperture (NA = 1.46) microscope objective. (b) Schematic showing the sample structure consisting of a gold thin film (40 nm thick) coated with 11 layers of PTCDI-C7 molecules. (c) Image of the back focal plane obtained by the LRM. Wavevector-resolved spectra are obtained by moving along the k_y=0 line a 4 μm core diameter optical fiber connected to a spectrometer.

under laser excitation at λ = 532 nm. For convenience in this experiment, the evaporation is realized on a transparent substrate. The absorption (blue) and emission (red) spectra of PTCDI-C7 molecules are plotted in Figure 2a and display a large Stokes shift of 75 nm. The absorption spectrum also displays a high-intensity, low-energy peak at 565 nm (FWHM = 20 nm), which is enhanced by a factor of 2 with respect to the one of the control sample (Figure 2b) consisting of molecules deposited on a low-temperature substrate (see the Methods section). The comparison with the spectrum of dispersed molecules shows that this peak is too much red-shifted relative to the main absorption to correspond to the 0−0 vibronic level of a PTCDI π-conjugated core. The high excitonic peak of the ordered sample is a typical signature of the formation of large oscillator strength charge-transfer Frenkel excitons in such $\pi-\pi$ stacked molecular aggregates.[19] Although the dipole−dipole interactions should strongly reduce the luminescence rate in this typical Kasha's H-aggregate geometry, it can be compensated by $\pi-\pi$ interaction,[20] as observed here. Moreover, the dipole of this transition being along the molecule main axis, coupling with the plasmon of predominantly vertical polarization is expected to be favored. Wavevector-resolved reflectance spectra are obtained in the back focal plane of the microscope objective thanks to the LRM setup.[14] The LRM technique can be considered as a generalized Kretschmann geometry, the objective and index-matching liquid playing the role of the prism, but with multiple incidences impinging simultaneously on the sample rather than one in the classical Kretschmann prism experiment. The periodic grating coupling/decoupling technique significantly alters the plasmon characteristics, whereas LRM preserves the characteristics of the open-cavity structure. Our imaging system is displayed in Figure 3a.

DOI: 10.1021/acs.jpclett.7b02586
J. Phys. Chem. Lett. 2017, 8, 5626−5632

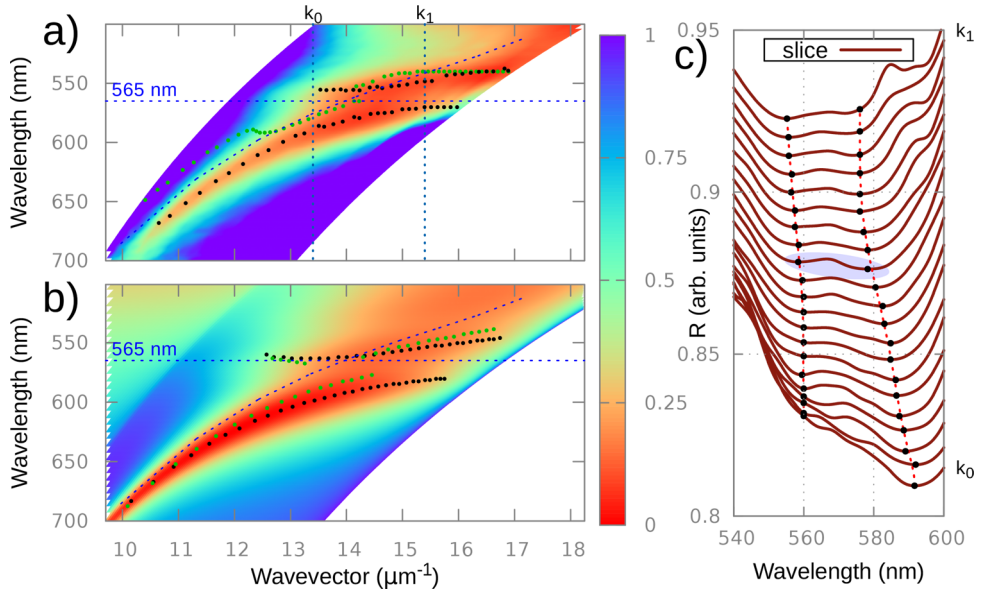

Figure 4. Reflectance cartography in the wavevector−wavelength plane measured experimentally for the coupled system and for ordered molecules (a) with reflectance minima (black dots). The reflectance minima experimentally measured for the reduced order molecular system are superimposed (green dots). The unperturbed exciton resonance is represented as a nondispersive line at a fixed wavelength of 565 nm, together with the dispersion line of the unperturbed SPP as computed with the organic layer replaced by a normally dispersive dielectric layer deprived of excitonic resonance. (b) Numerical reflectance cartography of the coupled system and reflectance minima (black dots) together with the uncoupled excitonic and SPP theoretical dispersions (blue dashed line). (c) Reflectance spectra for the wavevector between k_0 = 13.4 μm^{-1} and k_1 = 15.4 μm^{-1} in the case of ordered molecules. The spectra are translated vertically for clarity. Maximal photon−exciton mixing at k = 14.6 μm^{-1} (blue ellipse) leads to a clear anticrossing revealing a Rabi splitting of Ω_R = 102 meV for the ordered molecular system.

The back focal plane image displays the distribution of photon momenta and allows discrimination by their wavevectors in k-space. In other words, every point in this plane corresponds to a distinct angle of emission or reflection. To investigate the interactions between self-assembled molecules and SPPs in absorption, a transverse-magnetic (TM) white light beam (polarized along the k_y = 0 axis) is introduced in the LR microscopy setup. This technique allows the Rabi splitting to be determined from the spectrum in k-space, thus avoiding overestimating it.[7,21] The back focal plane image is presented in Figure 3c. The maximum collection angle θ_{max} = 74.5° is determined by the numerical aperture of the oil immersion objective (NA = 1.46). Besides, the back focal plane image shows two main contributions: the uniform central part and the intermediate part where absorption of our hybrid system occurs. By collecting absorption spectra at different positions (i.e., wavevectors) along the k_y = 0 axis with an optical fiber, we are able to establish the wavevector-resolved reflectance. The results for the 30 nmthick hybrid sample with ordered molecules is shown in Figure 4. 2D reflectance cartography, Figure 4a, reveals two branches of minimum reflectance. The two observed branches result from the coupling from a charge-transfer Frenkel exciton transition and the SPP mode. They are strongly hybridized and exchange their predominant excitonic or SPP nature at the anticrossing while being close to the uncoupled states far from it. To highlight the position of the branches, we have plotted with a dotted line the position of the reflectance minima along them for ordered molecules (black) and for the reduced order molecules (green), and we plotted with a dotted (blue) line the uncoupled exciton energy and the dispersion relation of the uncoupled SPP. As the reflectance angle increases, the excitonic branch is repelled from the SPP branch, resulting in an anticrossing, as plotted in Figure 4c. The anticrossing reveals the formation of hybrid exciton-plasmon coupled states and attests the strong coupling between the Franck−Condon exciton state and the SPP.[22] We measure the linewidth of the bare SPP mode to be γ_{SPP} = 68 meV (in good agreement with the calculated value of 60 meV) and the one of the excitonic mode to be γ_{dye} = 77 meV. We measure the Rabi splitting Ω_R = 102 meV at k = 14.6 μm^{-1}, where the widths of the two branches are equal. It satisfies the usually accepted condition for strong coupling[7] $\Omega_R \gtrsim \frac{\gamma_{SPP}}{2} + \frac{\gamma_{dye}}{2}$. The Rabi splitting is comparable with values reported with J-aggregate molecules in an open-cavity architecture.[1,23] No anticrossing has been observed for the higher-energy absorption band due to their large linewidth and relatively low oscillator strength compared to the excitonic peak of H-aggregates. By contrast, the reflectance minima obtained in the case of reduced order molecules cannot be tracked over the whole wavevector range because the two branches are not well-resolved. The lowest splitting between the branches is Ω_S = 60 meV at k = 14.2 μm^{-1}, which nevertheless does not satisfy the strong coupling condition. The strong coupling regime observed in ordered PTCDI-C7 molecules compared to that in reduced order dyes is attributed to the spectral concentration of oscillator strength, which is characteristic of collective oscillation modes and to the high density of such available modes in the small volume of the confined SPP field. In Figure 4b, we have performed numerical simulations with the transfer matrix method[24], where we consider the two-layer system SiO_2/Au/PTCDI-C7/Air (as described in the Methods section). Using the optical constants extracted from ellipsometry measurements and modeling with a perfect alignment of excitonic transition dipoles, good agreement is obtained between modeling and experiment. We note that both resonant (excitonic) and nonresonant optical constants affect the coupling strength (see the Methods section). We now investigate our hybrid system in emission

DOI: 10.1021/acs.jpclett.7b02586
J. Phys. Chem. Lett. 2017, 8, 5626−5632

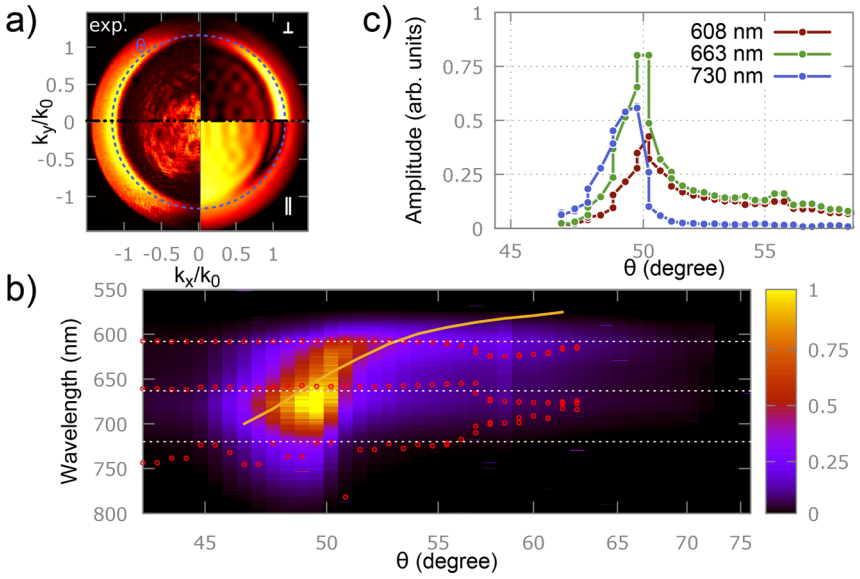

Figure 5. (a) Back focal plane image of the sample emission under laser excitation at λ = 532 nm: experiment (left) and FDTD simulation with a perpendicular (upper right) or parallel (lower right) dipole. (b) Wavevector-resolved emission spectrum with overlaid dispersion of a coupled SPP−molecule lower-energy state (orange line). Red circles are the emission line centers resulting from the fit of the emission spectrum at the given wavevector. The three main components of the bare molecule emission spectrum are shown by white dotted lines. (c) Amplitude of the fitted emission lines versus emission angle.

by wavevector-resolved emission spectra obtained in the same LRM setup. For this purpose, we collect emission in the back focal plane under 1 mW of λ = 532 nm laser excitation from the glass side. The photoluminescence spectra are analyzed in TM polarization. The angle-dependent emission measurements are shown in Figure 5c. We identify the angle-independent, free-space emission of the molecular assembly at the two main emission wavelengths of 608 and 663 nm. These lines correspond also to the photoluminescence spectrum recorded in a zone of the sample where the molecules are evaporated directly on glass. Visible intensification of emission occurs near θ = 50°. In Figure 5b, the three amplitudes of the fitted emission lines are shown in k-space and display a maximum at three distinct wavevectors. This observation corresponds to an enhancement occurring when the molecular assembly emits in the plasmon mode, i.e., approximately when the emission and the SPP dispersion cross, as shown in Figure 5b. Emission coupled to the SPP mode is favored by the vertical orientation of the dipoles, parallel the SPP electric field.[25] To assess the vertical orientation of the dipoles, we have performed rigorous finite difference time domain (FDTD) simulations[26] of the emission pattern in the back focal plane for dipoles perpendicular or parallel to the gold surface. The juxtaposition of simulation (left side) and experimental (right side) back focal plane images is presented in Figure 5a. We note that a bright ring appears near θ = 50° in the experiment and in the simulation only in the case of the perpendicular (upper right) dipole. In contrast to the reflectance experiment, the hybrid sample does not exhibit anticrossing at the emission frequency. The emission is therefore in the weak coupling regime. At our low pumping intensity, the excited molecules remain an extreme minority compared to ground-state ones. The strong resonance due to the transition from the ground state to the Franck−Condon state, which is at the origin of the strong coupling observed in absorption measurements above, is unchanged and manifests itself as a constant hybridized electromagnetic environment.

Because of the large Stokes shift, the luminescence is spectrally moved toward a much lower frequency, far from the corresponding anticrossing, and is thus coupled to a poorly hybridized branch of the surface plasmon. This is in striking contrast with systems presenting low Stokes shifts, which essentially behave as two-level systems. Here, we are mainly dealing with a four-level system presenting well-differentiated transitions for absorption from the ground state and emission from the excited state. As mentioned in the introduction, contrary to absorption, spontaneous emission is by nature a noncoherent process. Although at higher pumping rates stimulated emission and optical gain may restore some coherence, e.g., in amplified spontaneous emission (ASE), here the possibility of strong coupling with an excited-state Stokes-shifted transition relies on the sole oscillator strength of this transition. This excited state experiences complex photophysical behaviors,[27] leading to a relatively small oscillator strength of the lowest Frenkel state.[28,29] Despite the possible role of the plasmonic environment in mediating dipole−dipole interactions between remote molecules,[9,10] the dispersion curve observed in the emission regime does not permit one to conclude to strong coupling between a collective molecular excitation and the SPP. Actually, at our pumping intensity, the density of excited molecules remains negligible. Strong coupling between the SPP and Franck−Condon excitonic state observed by absorption is still present; however, because the numbers of excited Frenkel states is small, the Rabi splitting between the SPP and the Frenkel exciton is too small to be observed. This is in striking contrast with J-aggregates because the emission frequency is here Stokes-shifted away from the anticrossing between the SPP and the Franck−Condon exciton.

The weak coupling regime observed in emission with our molecular system is also in agreement with previously reported studies.[30,31] Large Stokes shift in molecules induce a faster dissipation of energy into the vibrational modes than the dephasing rate, which contributes to faster decay of the polariton state.

DOI: 10.1021/acs.jpclett.7b02586
J. Phys. Chem. Lett. 2017, 8, 5626−5632

To summarize, we have achieved condensed-phase films of self-assembled PTCDI-C7 dyes where the molecules stand perpendicularly to a gold thin film, without a host matrix. Using LR microscopy, wavevector-resolved reflectance measurements evidence the strong coupling regime between the SPP mode and the high oscillator strength molecular charge-transfer Frenkel exciton originating from the self-assembly-induced molecular $\pi-\pi$ stacking with a Rabi splitting of Ω_R = 102 meV. By contrast, we demonstrate that the use of organic films of PTCDI-C7 molecules with a reduced order does not lead to the strong coupling regime in absorption. The wavevector-resolved emission spectrum shows weak coupling of the relaxed exciton to the unperturbed SPP field. This is due to the large Stokes shift present in PTCDI-C7 H-aggregates that shifts the emission away from the anticrossing between the SPP and the Franck−Condon excited state. We believe that self-assembled molecular media are promising model systems to study the interaction between confined fields and dipoles at the nanoscale. The use of the self-assembly approach combined with molecular engineering opens interesting perspectives for the ultimate control of molecular dipole orientation to maximize interaction with the SPP field and for the control of the stacking geometry, which is crucial for the emission properties of the molecular system. It could also benefit to phenomena such as superradiant emission,[32] paving the road to promising applications.

METHODS

Sample Fabrication. A Thin gold film of 40 nm thickness is deposited onto a 170 μm thick BK7 coverslip. Commercial PTCDI-C7 powders are then evaporated in an ultrahigh vacuum chamber at a temperature of around 480 K, and the deposition regime is monitored by a quartz balance positioned near the substrate. For the first sample, the molecular flux is controlled in order to obtain a slow, monolayer by monolayer deposition on the gold thin film. The substrate is held at T_{sub} = 470 K, which results in around 11 layers of ordered molecules. For the second sample, we evaporate the same molecules on a substrate kept at room temperature to obtain a 30 nm thick layer of reduced order molecules. The excitonic peak at 565 nm, which is relative to the $\pi-\pi$ stacking of the molecules, is then greatly reduced, a fact that is related to the reduced ordering of the molecular self-assembly.

Experimental Setup. In the LRM investigation of absorption, the sample is back-illuminated by a white-light source (CoolLED pE-100wht). Light coming from the object plane is collected by an oil immersion objective of high numerical aperture (NA = 1.46) and forms an intermediary back focal plane, which can be imaged by adding a lens (focal length = 500 mm) at focal distance on a 2D charged-coupled device (CCD) and at the tip of an optical fiber. The optical fiber is connected to a spectrometer (Princeton Instruments) with a Pixis 400 eXcelon cooled CCD detector. The fiber core size (∼4 μm) and the back focal plane image size (2.8 mm) allow efficient discretization in k-space.

Numerical Simulations. Numerical reflectivity maps were calculated using homemade implementation of a S-matrix code that can handle uniaxial anisotropy. The simulated structure is made of a glass substrate (incident side), a 40 nm gold layer, a 30 nm molecular layer, and air. The glass permittivity is taken constant at ϵ = 1.5. Gold permittivity is modelled by a multiple resonator model[33] that fits Johnson and Christy data.[34] A PTCDI-C7 molecular layer is modeled by a four-oscillator model in the direction perpendicular to the interface, whose parameters are fitted to an experimental ellispometry measurement. In the parallel direction, a constant value of ϵ = 1.55 gives the best agreement with the experimental dispersion curve.

Calculations of the emission in the back focal plane are performed with the FDTD Lumerical package. A Hertzian dipole is positioned 2 nm above the 40 nm thick gold film on an infinite SiO_2 substrate. The near-field computed 50 nm below the gold surface is projected into the far-field to obtain the back focal plane image.

AUTHOR INFORMATION

Corresponding Author

*E-mail: sylvain.barbay@c2n.upsaclay.fr.

ORCID

F. Charra: 0000-0003-1228-0583

S. Barbay: 0000-0003-0092-7829

Notes

The authors declare no competing financial interest.

ACKNOWLEDGMENTS

The authors acknowledge the support of the French Agence Nationale de la Recherche (ANR) under Grant ANR-13-BS10-0006 (project SAMPLE). This work has been also supported by a joint Ph.D. funding from CEA and Triangle de la Physique and by a public grant overseen by the French National Research Agency (ANR) as part of the "Investissements d'Avenir" program (Labex NanoSaclay, reference: ANR-10-LABX-0035). The author would like to thank Ludovic Tortech for his helpful advices.

REFERENCES

(1) Bellessa, J.; Bonnand, C.; Plenet, J. C.; Mugnier, J. Strong Coupling between Surface Plasmons and Excitons in an Organic Semiconductor. *Phys. Rev. Lett.* **2004**, *93*, 036404.

(2) Sanvitto, D.; Kéna-Cohen, S. The Road Towards Polaritonic Devices. *Nat. Mater.* **2016**, *15*, 1061−1073.

(3) Schwartz, T.; Hutchison, J. A.; Genet, C.; Ebbesen, T. W. Reversible Switching of Ultrastrong Light-Molecule Coupling. *Phys. Rev. Lett.* **2011**, *106*, 196405.

(4) Kasprzak, J.; Richard, M.; Kundermann, S.; Baas, A.; Jeambrun, P.; Keeling, J. M. J.; Marchetti, F. M.; Szymańska, M. H.; André, R.; Staehli, J. L. Bose−Einstein Condensation of Exciton Polaritons. *Nature* **2006**, *443*, 409−414.

(5) Kelkar, P. V.; Kozlov, V. G.; Nurmikko, A. V.; Chu, C.-C.; Han, J.; Gunshor, R. L. Stimulated Emission, Gain, and Coherent Oscillations in II-VI Semiconductor Microcavities. *Phys. Rev. B: Condens. Matter Mater. Phys.* **1997**, *56*, 7564−7573.

(6) Saba, M.; Ciuti, C.; Bloch, J.; Thierry-Mieg, V.; André, R.; Dang, L. S.; Kundermann, S.; Mura, A.; Bongiovanni, G.; Staehli, J. L. High-Temperature Ultrafast Polariton Parametric Amplification in Semiconductor Microcavities. *Nature* **2001**, *414*, 731−735.

(7) Törmä, P.; Barnes, W. L. Strong Coupling Between Surface Plasmon Polaritons and Emitters: a Review. *Rep. Prog. Phys.* **2015**, *78*, 013901.

(8) Andreani, L. C.; Panzarini, G.; Gérard, J.-M. Strong-Coupling Regime for Quantum Boxes in Pillar Microcavities: Theory. *Phys. Rev. B: Condens. Matter Mater. Phys.* **1999**, *60*, 13276−13279.

(9) Pustovit, V. N.; Shahbazyan, T. V. Plasmon-mediated superradiance near metal nanostructures. *Phys. Rev. B: Condens. Matter Mater. Phys.* **2010**, *82*, 075429.

(10) George, J.; Wang, S.; Chervy, T.; Canaguier-Durand, A.; Schaeffer, G.; Lehn, J.-M.; Hutchison, J. A.; Genet, C.; Ebbesen, T. W.

DOI: 10.1021/acs.jpclett.7b02586
J. Phys. Chem. Lett. 2017, 8, 5626−5632

Ultra-strong coupling of molecular materials: spectroscopy and dynamics. *Faraday Discuss.* **2015**, *178*, 281−294.
(11) Charra, F., Agranovich, V. M., Kajzar, F., Eds. *Organic Nanophotonics, Nato Science Series II: Mathematics, Physics and Chemistry*; Springer Netherlands: The Netherlands, 2003; Vol. 100 10.1007/978-94-010-0103-8..
(12) Bléger, D.; Mathevet, F.; Kreher, D.; Attias, A.-J.; Bocheux, A.; Latil, S.; Douillard, L.; Fiorini-Debuisschert, C.; Charra, F. Janus-Like 3D Tectons: Self-Assembled 2D Arrays of Functional Units at a Defined Distance from the Substrate. *Angew. Chem., Int. Ed.* **2011**, *50*, 6562−6566.
(13) Le Liepvre, S.; Du, P.; Kreher, D.; Mathevet, F.; Attias, A.-J.; Fiorini-Debuisschert, C.; Douillard, L.; Charra, F. Fluorescent Self-Assembled Molecular Monolayer on Graphene. *ACS Photonics* **2016**, *3*, 2291−2296.
(14) Hohenau, A.; Krenn, J. R.; Drezet, A.; Mollet, O.; Huant, S.; Genet, C.; Stein, B.; Ebbesen, T. W. Surface Plasmon Leakage Radiation Microscopy at the Diffraction Limit. *Opt. Express* **2011**, *19*, 25749−25762.
(15) Kumar, M.; Kumar, S. Liquid crystals in Photovoltaics: a New Generation of Organic Photovoltaics. *Polym. J.* **2017**, *49*, 85−111.
(16) Ferguson, A. J.; Jones, T. S. Photophysics of PTCDA and Me-PTCDI Thin Films: Effects of Growth Temperature. *J. Phys. Chem. B* **2006**, *110*, 6891−6898.
(17) Proehl, H.; Dienel, T.; Nitsche, R.; Fritz, T. Formation of Solid-State Excitons in Ultrathin Crystalline Films of PTCDA: From Single Molecules to Molecular Stacks. *Phys. Rev. Lett.* **2004**, *93*, 097403.
(18) Struijk, C. W.; Sieval, A. B.; Dakhorst, J. E. J.; van Dijk, M.; Kimkes, P.; Koehorst, R. B. M.; Donker, H.; Schaafsma, T. J.; Picken, S. J.; van de Craats, A. M. Liquid Crystalline Perylene Diimides: Architecture and Charge Carrier Mobilities. *J. Am. Chem. Soc.* **2000**, *122*, 11057−11066.
(19) Spano, F. C. The Spectral Signatures of Frenkel Polarons in H- and J-Aggregates. *Acc. Chem. Res.* **2010**, *43*, 429−439.
(20) Hestand, N. J.; Spano, F. C. Molecular Aggregate Photophysics beyond the Kasha Model: Novel Design Principles for Organic Materials. *Acc. Chem. Res.* **2017**, *50*, 341−350.
(21) Symonds, C.; Bonnand, C.; Plenet, J. C.; Bréhier, A.; Parashkov, R.; Lauret, J. S.; Deleporte, E.; Bellessa, J. Particularities of Surface Plasmon-Exciton Strong Coupling with Large Rabi Splitting. *New J. Phys.* **2008**, *10*, 065017.
(22) Houdré, R. Early Stages of Continuous Wave Experiments on Cavity-Polaritons. *Phys. Status Solidi B* **2005**, *242*, 2167−2196.
(23) Hakala, T. K.; Toppari, J. J.; Kuzyk, A.; Pettersson, M.; Tikkanen, H.; Kunttu, H.; Törmä, P. Vacuum Rabi Splitting and Strong-Coupling Dynamics for Surface-Plasmon Polaritons and Rhodamine 6G Molecules. *Phys. Rev. Lett.* **2009**, *103*, 053602.
(24) Bienstman, P.; Baets, R. Optical Modelling of Photonic Crystals and VCSELs using Eigenmode Expansion and Perfectly Matched Layers. *Opt. Quantum Electron.* **2001**, *33*, 327−341.
(25) Li, Y. J.; Hong, Y.; Peng, Q.; Yao, J.; Zhao, Y. S. Orientation-Dependent Exciton- Plasmon Coupling in Embedded Organic/Metal Nanowire Heterostructures. *ACS Nano* **2017**, *11*, 10106.
(26) Lumerical Solutions, Inc. http://www.lumerical.com/tcad-products/fdtd/ (2017).
(27) Sung, J.; Kim, P.; Fimmel, B.; Würthner, F.; Kim, D. Direct observation of ultrafast coherent exciton dynamics in helical π-stacks of self-assembled perylene bisimides. *Nat. Commun.* **2015**, *6*, 8646.
(28) Spano, F. C.; Silva, C. H- and J-Aggregate Behavior in Polymeric Semiconductors. *Annu. Rev. Phys. Chem.* **2014**, *65*, 477−500.
(29) Schuller, J. A.; Karaveli, S.; Schiros, T.; He, K.; Yang, S.; Kymissis, I.; Shan, J.; Zia, R. Orientation of Luminescent Excitons in Layered Nanomaterials. *Nat. Nanotechnol.* **2013**, *8*, 271−276.
(30) Koponen, M. A.; Hohenester, U.; Hakala, T. K.; Toppari, J. J. Absence of Mutual Polariton Scattering for Strongly Coupled Surface Plasmon Polaritons and Dye Molecules with a Large Stokes Shift. *Phys. Rev. B: Condens. Matter Mater. Phys.* **2013**, *88*, 085425.
(31) Baieva, S.; Hakamaa, O.; Groenhof, G.; Heikkilä, T. T.; Toppari, J. J. Dynamics of Strongly Coupled Modes between Surface Plasmon Polaritons and Photoactive Molecules: The Effect of the Stokes Shift. *ACS Photonics* **2017**, *4*, 28−37.
(32) Choquette, J. J.; Marzlin, K.-P.; Sanders, B. C. Superradiance, Subradiance, and Suppressed Superradiance of Dipoles near a Metal Interface. *Phys. Rev. A: At., Mol., Opt. Phys.* **2010**, *82*, 023827.
(33) Etchegoin, P. G.; Le Ru, E. C.; Meyer, M. An Analytic Model for the Optical Properties of Gold. *J. Chem. Phys.* **2006**, *125*, 164705.
(34) Johnson, P. B.; Christy, R. W. Optical Constants of the Noble Metals. *Phys. Rev. B* **1972**, *6*, 4370−4379.

DOI: 10.1021/acs.jpclett.7b02586
J. Phys. Chem. Lett. 2017, 8, 5626−5632